Characterization of temperature and pH-responsive poly-N-isopropylacrylamide-co-polymer nanoparticles for the release of antimicrobials

2014 Mater. Res. Express 1 035405

(http://iopscience.iop.org/2053-1591/1/3/035405)

Materials Research
Express

Characterization of temperature and pH-responsive poly-N-isopropylacrylamide-co-polymer nanoparticles for the release of antimicrobials

Laura E Hill and Carmen L Gomes

Department of Biological & Agricultural Engineering, Texas A&M University College Station, TX–77843-2117, USA
E-mail: carmen@tamu.edu

Received 29 June 2014, revised 21 August 2014
Accepted for publication 1 September 2014
Published 25 September 2014

Materials Research Express **1** (2014) 035405

doi:10.1088/2053-1591/1/3/035405

Abstract

Chitosan and alginate are both pH-responsive biopolymers extracted from crustacean exoskeletons and brown algae, respectively. Poly-N-isopropylacrylamide (PNIPAAM) is a hydrogel that becomes hydrophobic at a lower-critical solution temperature. This study sought to combine pH- and temperature-responsive polymers via crosslinking, in order to create a dual-stimuli responsive polymer for hydrophobic antimicrobial compounds delivery, improving their antimicrobial effects. Cinnamon bark extract (CBE) was used as a model for hydrophobic antimicrobial. Two co-polymers were synthesized to create two nanoparticles types: chitosan-co-PNIPAAM and alginate-co-PNIPAAM. Nanoparticles were formed from the resulting co-polymers using a self-assembly top-down process followed by glutaraldehyde or calcium chloride crosslinking. These nanoparticles were then used as controlled delivery vehicles for CBE, whose rapid release could be triggered by specific external stimuli. For the same pH and temperature conditions, the chitosan-co-PNIPAAM nanoparticles were significantly more potent bacterial inhibitors against both pathogens and also exhibited a faster CBE release over time as well as slightly higher entrapment efficiency. The alginate-co-PNIPAAM nanoparticles were significantly smaller and exhibited a slow, gradual release over a long time period. Although both nanoparticles were able to effectively inhibit pathogen growth at lower ($P < 0.05$) concentration than free CBE, the chitosan-co-PNIPAAM nanoparticles were more effective in delivering a natural antimicrobial with controlled release against foodborne pathogens.

Keywords: dual stimuli-responsive, hydrophobic antimicrobial, nano-encapsulation, antimicrobial controlled release, chitosan, alginate

1. Introduction

Chitosan and alginate are biodegradable polymers that respond to fluctuations in pH. Chitosan is extracted from the exoskeletons of crustaceans and has a pKa of 6.2, meaning it is positively charged in acidic to neutral solution and readily binds to negatively charged surfaces [1]. At this pH chitosan shifts from being hydrophilic at pH below the pKa value to hydrophobic at pH values above its pKa [2, 3]. Chitosan is a long-chained molecule, and when it becomes hydrophobic, it contracts to minimize thermodynamically unfavorable interactions. Alginate exhibits similar behavior, but at opposing pH ranges. It is an anionic polysaccharide extracted from brown algae and has a pKa of approximately 3.5 [4, 5]. Above the pKa, alginate is hydrophilic and in environments that are below this pH, alginate is hydrophobic.

These polymers can be crosslinked with PNIPAAM, which responds to temperature stimuli, to create a dual-stimuli responsive polymer. Poly(N-isopropylacrylamide) (PNIPAAM) reacts reversibly at a lower critical solution temperature (LCST) that ranges from 30–35 °C [6]. PNIPAAM's structure possesses hydrophilic and hydrophobic groups within its polymer chain which enables its temperature responsive behavior at the LCST [7]. Hydrogen-bonds form between water and the hydrophilic groups of the polymer at temperatures below the LCST, which results in a swollen hydrogel PNIPAAM. As the polymer is subjected to temperatures above the LCST, a weakening of the polymer-water hydrogen bonds occurs and the polymer to polymer interactions among the hydrophobic groups predominate [8]. Once temperatures are increased above the LCST, the polymer becomes hydrophobic and its polymer chains contract to minimize thermodynamically unfavorable interactions between the aqueous environment and the hydrophobic polymer groups [6, 8].

These alginate-PNIPAAM and chitosan-PNIPAAM co-polymers can then be used to encapsulate antimicrobial essential oils in order to control their release using environmental stimuli, both temperature and pH, and ultimately improve their efficacy. These co-polymers will contract in response to the external stimuli that induce hydrophobic behaviors. This polymer contraction (of one or both components of the co-polymers) will force out some of the active material entrapped within the polymer matrix, creating a burst release at the transition temperature or pH [9]. The temperature range for PNIPAAM's LCST is similar to the optimal temperature range for microbial growth for several foodborne pathogens of interest, while the desired pH range for release can be designed by selecting either alginate or chitosan as the co-polymer. Although there have been several previous studies on the antimicrobial capabilities of essential oils [10, 11], there has not been any previously reported work on developing a stimuli-responsive controlled release of antimicrobials for the food industry.

Cinnamon bark extract (CBE) is a highly effective antimicrobial of natural origin, which could provide a 'label-friendly' way to inhibit bacterial growth and prevent foodborne pathogen outbreaks; however, it has a very low aqueous solubility and high volatility that limit its contact with foodborne pathogens which favor aqueous environments [12, 13]. Nanoencapsulation provides protection to the cinnamon extract and allows for careful design and control of the antimicrobial release. Essential oils have extremely low flavor thresholds, so care must be taken to minimize the amount added to food products [14]. Encapsulation helps mask the sensory impact and also decreases the effective inhibitory concentration by increasing CBE solubility and improving its delivery to pathogen sites.

A stimuli-responsive polymer could create a way to trigger an antimicrobial release when foods are stored at a pH or temperature that promotes microbial growth. Antimicrobials would

be released when they are needed the most, rather than being metabolized or degraded before they are in contact with pathogenic bacteria. While there have been numerous studies on the use of PNIPAAM, alginate, or chitosan to develop nanoparticle delivery systems as vehicles for delivery of pharmaceuticals; however, these polymers have not previously been studied to create a dual-stimuli responsive nanoparticle as vehicles for delivery of antimicrobial compounds for food applications. Furthermore, no previous studies have synthesized nanoparticles from alginate-PNIPAAM. Moreover, thus far there have been no research studies comparing the response of alginate-PNIPAAM hydrogels to chitosan-PNIPAAM hydrogel materials. The goal of this study is to develop a stimuli-responsive nanoparticle system to more effectively inhibit bacteria growth and reduce the incidence of foodborne pathogen related illnesses associated with improper food handling or storage.

No previous studies have synthesized nanoparticles from alginate-PNIPAAM.

2. Materials and methods

2.1. Materials

N-isopropylacrylamide (NIPAAM) was purchased from TCI America (Portland, OR). Poly (vinyl alcohol) (PVA) (87%, M_w 30–70 kDa), chitosan (M_w 190–310 kDa, 75–85% deacetylated chitin, viscosity ⩽30 mPa s), sodium alginate (M_w 120–190 kDa, mannuronate/gluronate (M/G) ratio = 1.56), N,N-methylene-bisacrylamide (MBA), glutaraldehyde (25%), and CBE (99%) were purchased from Sigma Aldrich (St. Louis, MO). N,N,N',N'-tetramethyl-ethylenediamine (TEMED) was purchased from Alfa Aesar (Ward Hill, MA). Ammonium persulfate (APS) was purchased from BDH Chemicals (London, England). All other reagents were of analytical grade.

2.2. Particle synthesis

2.2.1. Alginate co-polymer synthesis. Alginate-PNIPAAM polymer was synthesized by a semi-IPN (interpenetrating polymer network) method similar to that outlined by Moura *et al* [15] and Zhang *et al* [16]. First, 8 g of NIPAAM monomer were dissolved in 100 mL of distilled water with 3% (w/w) sodium alginate, relative to NIPAAM. To this solution, 2% (w/w) N,N'-methylenebisacrylamide (MBA) was added as a crosslinker, followed by 1% (w/w) ammonium persulfate (APS) and 1% (w/w) TEMED to serve as redox initiators. Polymerization took place at 5 °C for 24 h in a glass vessel without any agitation, then the polymer was cut into small pieces and immersed in an excess of distilled water to remove residual monomers and reactants. The water was replaced with fresh distilled water every few hours over a 24 h period. The hydrogel was then dried in a vacuum oven (Squared Lab Line Instruments, Melrose Park, IL) at room temperature and a pressure ⩽13.3 kPa to remove all moisture. The dried polymer was stored at −20 °C until needed for particle synthesis.

2.2.2. Chitosan co-polymer synthesis. Chitosan-PNIPAAM polymer was prepared using a semi-IPN method similar to the method utilized by Lee *et al* [17] and Lee and Chen [18]. Briefly, a 1 M solution of NIPAAM (10 mL) was mixed with 3% (w/w, based on total monomers) chitosan in 1% (w/w) acetic acid until the chitosan had completely dissolved. Then, 3 mol% MBA (based on total monomers) was added to the solution, followed by 1% (w/w)

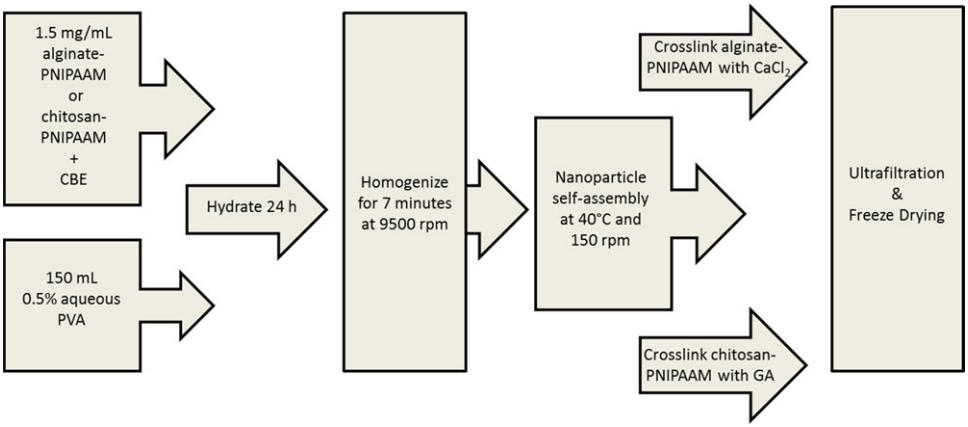

Figure 1. Schematic diagram of the self-assembly synthesis procedure for alginate-PNIPAAM or chitosan-PNIPAAM nanoparticles.

APS and TEMED. This solution was poured into a shallow glass dish and allowed to polymerize at 5 °C for 24 h. The crosslinked hydrogel was soaked in distilled water for 24 h, replacing the water with fresh water several times to remove any unreacted monomer. Following this purification process, the polymer was dried in a vacuum oven at room temperature for 24 h. Dried polymer was stored at −20 °C until needed for particle synthesis.

2.2.3. Particle synthesis. A similar procedure was used to form both types of nanoparticles (figure 1). First, 1.5 mg mL^{-1} of dried PNIPAAM-co-polymer was suspended in 150 mL of 0.5% (w/v) aqueous PVA solution with (16% (w/v)) or without CBE (without for control particles) and allowed to hydrate overnight without agitation. Following polymer hydration, the solution was homogenized using an Ultra-Turrax T25 basic Ika (Works, Wilmington, NC) at 9500 rpm for 7 min in order to break the polymer into smaller particles. After homogenization, the solutions were placed in a shaking water bath (VWR International, Radnor, PA) at 40 °C and 150 rpm for 24 h to allow the polymer to self-assemble into micelles. The chitosan-PNIPAAM and alginate-PNIPAAM micelles were then crosslinked with glutaraldehyde (2:1 molar ratio of glutaraldehyde to monomers) or calcium chloride (1% (w/v)), respectively, to generate IPN nanoparticles. The finished particles were then purified via ultrafiltration using a Millipore-Labscale TFF system fitted with a 50 kDa molecular weight cutoff Pellicon XL-Millipore (Millipore, Kankakee, IL) to remove excess reactants and free cinnamon extract. The nanoparticles were ultrafiltered with an inlet pressure of 25 psi and outlet pressure of approximately 5–10 psi, using 300 mL of water and 100 mL of the retentate was collected. After filtration, the particles were lyophilized at −50 °C and $1.45 \times 10 - 4$ psi vacuum for 24 h in a Labconco Freeze Dry-5 unit (Labconco, Kansas City, MO). Dried nanoparticles were stored at −20 °C until they were needed for analysis.

2.3. Particle characterization

2.3.1. Particle size and morphology. Aqueous suspensions of each nanoparticle were analyzed for size distribution and polydispersity index (PDI) using a Delsa Nano C Particle Analyzer (Beckman Coulter, Brea, CA). Nanoparticles were suspended in distilled water (neutral pH) at a concentration of 50 mg mL^{-1} and sonicated at 70 W (Cole Parmer sonicator 8890, Vernon Hill,

IL) for 15 min prior to analysis using 1 cm path length plastic cuvettes at a scattering angle of 165°, with a pinhole set to 50 μm, and a refractive index of 1.3328 for 120 continuous accumulation times. Particle size attributes were analyzed at 25 °C and 40 °C to observe the impact of heating the particles above the LCST.

Aqueous suspensions of nanoparticles were viewed using a FEI Morgagni Transmission Electron Microscope (TEM) (FEI Company, Hillsboro, OR) at the School of Veterinary Medicine and Biomedical Sciences of Texas A&M University (College Station, TX). All particles were viewed at room temperature (below the LCST) and neutral pH, due to equipment and material limitations. The microscope employed was not capable of maintaining elevated temperatures, so the reversible nature of the polymer transition at the LCST prevents viewing at different temperatures. Suspended particles were placed on 300 mesh copper grids and stained with a 2% (w/v) uranyl acetate aqueous stain (Electron Microscopy Sciences, Hatfield, PA) to provide contrast under magnification. Excess liquid on the mesh was removed with filter paper and the grid was allowed to dry before viewing under 100 00 to 100 000 times magnification. Observations were performed at 80 kV.

2.3.2. Entrapment efficiency (EE) and drug loading (DL). The entrapment efficiency of and drug loading of each nanoparticle were measured indirectly by determining the amount of CBE that was present in the permeate collected during ultrafiltration. It was assumed that any CBE that did not pass through the filter membrane was entrapped within particles. The amount of CBE present in the permeate was measured spectrophotometrically at 280 nm (Shimadzu UV-1601 spectrophotometer, Columbia, MA) in a 1 cm path length quartz cuvette. The EE and DL were calculated according to equations (1) and (2), respectively [19, 20]:

$$\mathrm{EE} = \frac{\text{amount of active compound entrapped}}{\text{initial active compound amount}} \times 100. \tag{1}$$

$$\mathrm{DL} = \frac{\text{amount of active compound entrapped}}{\text{amount of particles produced}} \times 100\ . \tag{2}$$

2.3.3. Cloud point and LCST. The LCST values of the PNIPAAM, chitosan-PNIPAAM, and alginate-PNIPAAM hydrogels were measured using differential scanning calorimetry in a Pyris 6 Perkin Elmer instrument (Pyris 5.0 Software, Boston, MA). Hydrogel samples were submerged in water (neutral pH) and allowed to swell to equilibrium before DSC measurements were taken. Roughly 10 mg of swollen PNIPAAM was placed into 40 μL aluminum pans and sealed with one hole in their lids and scanned from 25 °C to 50 °C at a rate of 3 °C per minute under nitrogen atmosphere [21]. The onset of the endothermal peak was considered the LCST.

The cloud point method [22] was used to find the thermal transition temperature of the control and CBE encapsulating co-polymer nanoparticles. A 0.1% (w/w) aqueous solution of particles (neutral pH) was prepared for each type of nanoparticle and three wells of a 96-well plate were filled with 200 μL of each nanoparticle suspension. Absorbance of the particle solutions was measured at 450 nm using a 96-well plate reader equipped with temperature control (VERSAmax Tunable Microplate Reader, Molecular Devices, Sunnyvale, CA). The cloud point was defined as the inflection point on a plot of absorbance versus temperature for each nanoparticle suspension as the temperature was increased from 25 °C to 50 °C at a rate of

2 °C every 10 min. The cloud point of the PNIPAAM-co-polymer hydrogels were also measured to ensure the cloud point method and DSC method produced comparable results.

2.3.4. Controlled release. Controlled release experiments were conducted at 25 °C, 35 °C, and 45 °C to determine the rate of CBE release below, above, or near the LCST of the particles. The release was measured at these temperatures in release media of pH 3 and pH 7.4 to determine the particle response to differing pH stimuli because chitosan and alginate are pH-responsive. Nanoparticles were suspended in phosphate buffered saline (PBS, 0.15 M, pH 3 or 7.4) to achieve a 1.0 mg mL^{-1} concentration of particles (sink conditions) in 15 mL conical tubes. The pH of the acidic PBS was adjusted with 0.5 M hydrochloric acid. The particle suspensions were placed in a shaking water bath (VWR International, Radnor, PA) set at 100 rpm and the desired temperature. At predetermined time intervals, 1 mL samples were removed and centrifuged at 23 506 g for 15 min to precipitate any nanoencapsulant material prior to spectrophotometric analysis of the supernatant at 280 nm.

The controlled release profile could be modeled by a semi-empirical equation (3) described by Korsmeyer *et al* [23] that accounts for both Fickian diffusion and transport due to swelling effects (termed 'non-Fickian Type II transport'):

$$\frac{M_t}{M_\infty} = kt^n \,, \tag{3}$$

where M_t/M_∞ is the percent of antimicrobial released at time t (s), k is a rate constant (1 s^{-1}), and n is the diffusional exponent (dimensionless). The release mechanism from swellable particles differs from a purely Fickian model since the release is governed by the polymer's swelling behavior as well as the diffusion rate of the antimicrobial through the polymer matrix [24].

2.4. Minimum inhibitory and bactericidal concentration (MIC and MBC)

2.4.1. Bacterial cultures. *Salmonella enterica* serovar Typhimurium LT2 and *Listeria monocytogenes* strain Scott A were obtained from Texas A&M University Food Microbiology Laboratory (College Station, TX). *S. typhimurium* and *L. monocytogenes* were resuscitated in tryptic soy broth (TSB) and tryptose phosphate broth (TPB) (Becton, Dickinson and, Sparks, MD), respectively, by two identical consecutive transfers and incubating for 24 h aerobically at 35 °C. The bacterial cultures were maintained on TSA and TSAYE (TSA containing 0.6% (w/v) yeast extract) slants stored at 4 °C for no more than three months for *S. typhimurium* and *L. monocytogenes*, respectively. Transfers from slants were conducted similarly to the resuscitation method to prepare microorganisms for analysis.

2.4.2. Antimicrobial activity. Minimum inhibitory concentrations (MICs) for the Chitosan-PNIPAAM and Alginate-PNIPAAM nanoparticles were measured using a broth dilution assay [25]. Growth curves for each strain were performed at 35 °C to correlate plate counts with optical density values at 630 nm (OD630) measured with an Epoch microplate spectrophotometer (BioTek Instruments, Winooski, VT). Bacterial inocula were incubated 20–22 h and then serially diluted in double-strength TSB (2x TSB) or TPB (2x TPB), as appropriate, to achieve an initial inoculum of approximately 3.0 $\log_{10}$ CFU/mL in each sample well while providing the appropriate amount of nutrients upon dilution. Initial inocula were

enumerated via spread plating on tryptic soy agar (TSA) or Modified Oxford agar (MOX) for *S. typhimurium* and *L. monocytogenes*; respectively, and incubated for 24 h at 35 °C. Aliquots of 100 μL of all antimicrobial solutions and solvent blanks were spread plated on TSA at the beginning of the experiment to ensure their sterility.

The MIC experiments were carried out in 96 well microtiter plates (sterilized 300 μl capacity—MicroWell, NUNC, Thermo-Fisher Scientific, Waltham, MA). The nanoparticles were placed in the microtiter plates as aqueous suspensions in concentrations ranging from 5000 to 25 000 μg mL^{-1} for both pathogens. Equal volumes (100 μL) of nanoparticle solution and bacterial inoculum in 2x broth were loaded into each test well. Negative controls were prepared with nanoparticle solutions and sterile 2x broth to account for baseline OD630 readings. Positive controls were also prepared containing inoculum and sterile distilled water or control nanoparticles to ensure nanoparticle encapsulate materials had no inhibitory effect on bacterial growth. Once all solutions were added to the plates, they were covered with a mylar plate sealer (Thermo Fisher Scientific), shaken gently, and OD630 of the wells was read (0 h). The microtiter plates were incubated (24 h at 35 °C) and shaken gently before OD630 readings were taken again to observe bacterial growth or inhibition in the presence of the nanoparticles over the course of the typical bacterial growth cycle. Antimicrobial test wells that showed $\leqslant$0.05 change in OD630 after 24 h of incubation were considered 'inhibited' by the antimicrobial (after appropriate baseline adjustments) for that time period. The MIC for each nanoparticle and pathogen was considered to be the lowest concentration of antimicrobial that inhibited growth for all test replicates [25].

Any wells that exhibited inhibition of the test microorganism after 24 h were then tested for bactericidal activity by spreading 100 μL from each well onto TSA and MOX plates for *S. typhimurium* and *L. monocytogenes*; respectively, and incubating for 24 h at 35 °C. If no colonies were observed on the plate surfaces following incubation for all replicates, the treatment concentration was considered bactericidal. The lowest concentration of nanoparticles demonstrating bactericidal activity across all replicates was considered the MBC.

2.5. Statistical analysis

All determinations were made in triplicate as independent experiments. All statistical analyses were performed using JMP v. 9 Software (SAS Institute, Cary, NC). Differences between variables were tested for significance using one-way analysis of variance (ANOVA) and significantly different means ($P < 0.05$) were separated using Tukey's Honestly Significant Differences (HSD) test. Controlled release data were fit to model using JMP software and the nonlinear modeling procedure to determine rate constants (k) and diffusional coefficients (n). The model constants were analyzed for goodness of fit using the nonlinear procedure to determine coefficients of determination (R^2).

3. Results and discussion

3.1. Particle characterization

3.1.1. Particle size and morphology. The morphology of both the alginate and chitosan-PNIPAAM nanoparticles appeared to be amorphous structures in TEM images (figure 2). The chitosan-PNIPAAM particles were larger ($P < 0.05$) chained structures, as anticipated,

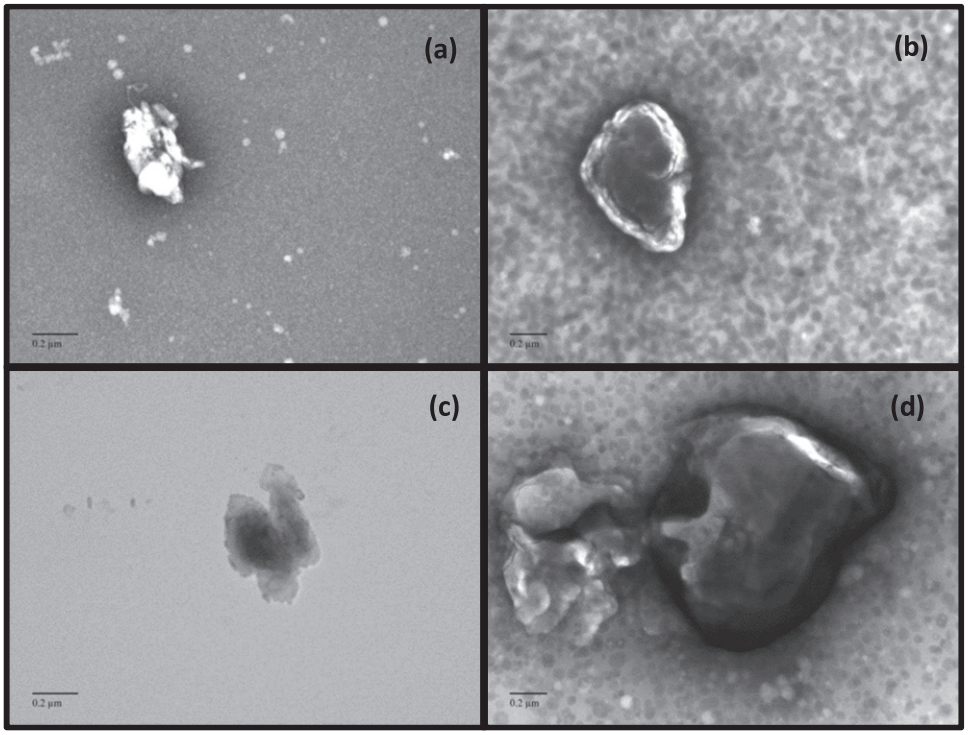

Figure 2. Transmission electron microscope (TEM) images of PNIPAAM-co-polymer nanoparticles. (a) Alginate-PNIPAAM control (unloaded); (b) alginate-PNIPAAM CBE; (c) chitosan-PNIPAAM control; (d) chitosan-PNIPAAM CBE. Observations were performed at 80 kV using magnifications ranging from 36 000 to 44 000×.

considering the large structure of chitosan polymers. The chitosan used in this study possesses a medium range molecular weight for chitosan polymers, ranging from 190–310 kDa and a high degree of deacetylation (75–85%). Alginate has a significantly smaller molecular size ranging from 120–190 kDa, leading to smaller polymer nanoparticles, as seen in previous study of chitosan and alginate nanoparticles [26].

Particle size analysis also showed the alginate-PNIPAAM nanoparticles to be significantly smaller than the chitosan-PNIPAAM nanoparticles (table 1) at temperatures above and below the LCST for each particle (loaded and unloaded with CBE), much like the TEM images. For both alginate-PNIPAAM and chitosan-PNIPAAN nanoparticles, the unloaded control particles were smaller in diameter than their CBE-containing counterparts at temperatures above the LCST. This phenomenon occurred because the polymers contract and collapse the micelles when heated above their LCST, and the unloaded nanoparticles had no CBE to prevent total collapse of the micelles [27].

All particle suspensions were found to have a heterogeneous particle size distribution, reflected in the PDI values greater than 0.1. The TEM images also demonstrated the wide range of particle sizes present in the alginate-PNIPAAM and chitosan-PNIPAAM particle solutions. The chitosan-PNIPAAM nanoparticles synthesized by [27] also showed a wide particle size distribution; however, their average diameter was smaller than the chitosan-PNIPAAM particles synthesized in this study. No previous studies have synthesized nanoparticles from alginate-PNIPAAM, they have only investigated the bulk alginate-PNIPAAM hydrogel [15, 28, 29].

Table 1. Comparison of average particle diameter and polydispersity index (PDI) for control (unloaded) and CBE entrapped alginate-PNIPAAM and chitosan-PNIPAAM nanoparticles below (25 °C) and above the LCST (40 °C).

	Average diameter (nm)		PDI	
Particle	25 °C	40 °C	25 °C	40 °C
Chitosan-PNIPAAM Control	$_{w}7526.80^{a} \pm 84.29$	$_{x}3179.58^{a} \pm 1703.13$	$_{w}0.81^{ab} \pm 1.04$	$_{w}0.48^{a} \pm 0.03$
Chitosan-PNIPAAM CBE	$_{w}9920.18^{a} \pm 3927.58$	$_{x}4580.40^{a} \pm 496.11$	$_{w}0.57^{b} \pm 0.30$	$_{w}0.54^{a} \pm 0.13$
Alginate-PNIPAAM Control	$_{w}110.07^{c} \pm 46.30$	$_{w}69.42^{c} \pm 15.67$	$_{w}1.15^{a} \pm 0.04$	$_{x}0.15^{b} \pm 0.05$
Alginate-PNIPAAM CBE	$_{w}955.78^{b} \pm 33.07$	$_{w}918.79^{b} \pm 71.57$	$_{w}1.08^{a} \pm 0.02$	$_{x}0.49^{ab} \pm 0.43$

Values given are averages of three replicates ± standard deviations. [a]Means within a column that are not followed by a common superscript letter are significantly different ($P < 0.05$). $_{w}$Means within a row, of the same parameter, that are not preceded by a common subscript letter are significantly different ($P < 0.05$).

Table 2. Entrapment efficiency and drug loading values measured for cinnamon bark extract (CBE) in chitosan- and alginate- PNIPAAM nanoparticles by spectrophotometry at 280 nm.

Nanoparticle	Entrapment efficiency (%)	Drug loading (%)
Chitosan-PNIPAAM CBE	$75.58^{a} \pm 9.46$	$1.93^{a} \pm 0.24$
Alginate-PNIPAAM CBE	$74.50^{a} \pm 8.13$	$1.07^{b} \pm 0.12$

Values given are averages of three replicates ± standard deviations. [a]Means within a column that are not followed by a common superscript letter are significantly different ($P < 0.05$).

3.1.2. Entrapment efficiency and drug loading. The entrapment efficiency was slightly higher in the chitosan-PNIPAAM nanoparticles than the alginate-PNIPAAM nanoparticles, but not significantly higher (table 2). Although the level of entrapment was similar, the chitosan particles were more effective bacterial inhibitors. Similar entrapment efficiencies were not surprising because both biopolymers were co-polymerized with PNIPAAM and self-assembly was conducted at the same temperature and pH for both co-polymers. Fan *et al* [27] found slightly lower values of entrapment efficiency and drug loading of a hydrophobic drug in chitosan-PNIPAAM nanoparticles synthesized via a similar method, while Chuang *et al* [30] found even lower values of EE and DL for a hydrophilic drug in a similar chitosan-PNIPAAM nanoparticle. Shi *et al* [31] synthesized alginate-PNIPAAM spheres encapsulating a hydrophobic drug at similar levels of EE and DL; however, these spheres were much larger than nano-scale delivery systems. PNIPAAM is the temperature-responsive component of the co-polymers, so its response to the temperature above the LCST during the self-assembly process governed the formation of the particle micelles and the entrapment of the CBE within the capsules. The elevated temperature during the self-assembly process caused the PNIPAAM to contract and form micelles around the hydrophobic CBE to minimize unfavorable interactions with the aqueous environment.

The alginate-PNIPAAM and chitosan-PNIPAAM nanoparticles presented high DL values, as they did with the entrapment efficiency values. A drug loading of 100% CBE entrapment would be 2.56% for the alginate-PNIPAAM nanoparticles and 1.43% for the chitosan-PNIPAAM nanoparticles, meaning the drug loading values for each of the particles were close to their maximum values. The drug loading maximum is higher for the alginate-PNIPAAM nanoparticles due to the higher M_w of chitosan.

3.1.3. Cloud point and LCST. The LCST for PNIPAAM hydrogel was measured in a previous study and fell within the typical range (30–35 °C) for PNIPAAM polymers at 33.9 °C via DSC determination [6]. The LCST of the alginate-PNIPAAM and chitosan-PNIPAAM hydrogels also fell within this range, at 32.5 °C and 31.2 °C, respectively. The LCSTs determined by the cloud point method were slightly higher at 33.8 °C for alginate-PNIPAAM and 34.2 °C for chitosan-PNIPAAM (table 3). The small differences in the LCST values determined by each method are attributable to the lower sensitivity of the cloud point method [32]. The cloud method allowed for larger aliquots of particle suspensions, enabling consistent LCST measurements. Eeckman *et al* [32] measured the cloud point and LCST values of PNIPAAM polymer, and found similar transition temperature values, irrespective of the method used to measure it and the values were similar to those reported for the nanoparticles in this study. The alginate-PNIPAAM control particles had the lowest LCST at 31.8 °C, while the alginate-

Table 3. Cloud point and lower critical solution temperatures (LCSTs) of chitosan- and alginate-PNIPAAM hydrogel and nanoparticles (control and CBE loaded).

Material	Cloud point (°C)	LCST (°C)
Alginate-PNIPAAM hydrogel*	$_{w}33.8^{ab} \pm 0.65$	$_{z}32.45 \pm 0.55$
Alginate-PNIPAAM control	$31.8^{c} \pm 0.78$	—
Alginate-PNIPAAM CBE	$32.6^{bc} \pm 0.29$	—
Chitosan-PNIPAAM hydrogel*	$_{w}34.2^{ab} \pm 0.78$	$_{z}31.16 \pm 0.47$
Chitosan-PNIPAAM control	$33.9^{ab} \pm 0.61$	—
Chitosan-PNIPAAM CBE	$34.7^{a} \pm 0.50$	—

Values given are averages of three replicates ± standard deviations. [a]Means within a column that are not followed by a common superscript letter are significantly different ($P < 0.05$). $_{w}$Means within a row that are not preceded by a common subscript letter are significantly different ($P < 0.05$). *Hydrogels consist of the bulk co-polymer materials synthesized before being used to manufacture nanoparticles.

PNIPAAM CBE nanoparticles had a slightly higher LCST value at 32.6 °C. Dumitriu *et al* [29] measured a similar range of LCST values for alginate-PNIPAAM hydrogels, that varied based upon the amount of alginate present in the polymer matrix. The chitosan-PNIPAAM control and CBE particles had slightly higher LCST values, at 33.9 °C and 34.7 °C, respectively. Chitosan-PNIPAAM hydrogels synthesized by Verestiuc *et al* [33] showed a similar transition temperature within the typical range for PNIPAAM polymers. None of the co-polymers or nanoparticles exhibited transition temperatures drastically different than the PNIPAAM hydrogel. The PNIPAAM is the temperature-responsive element of these co-polymers, so this behavior should not deviate significantly from the temperature response of PNIPAAM itself.

3.1.4. Controlled release. The release profiles of both the alginate and chitosan-co-PNIPAAM nanoparticles (figures 3(A) and (B)) were highly dependent upon the release media conditions, as was anticipated. For the chitosan-PNIPAAM particles, the release was governed primarily by temperature, while the release for the alginate-PNIPAAM particles was more heavily dependent upon the pH of the release media. The fact that the alginate-PNIPAAM nanoparticles respond more dramatically to changes in pH would lead us to believe that the co-polymer that comprises these particles has a higher level of alginate present in the co-polymer matrix. Conversely, the observation that the chitosan-PNIPAAM nanoparticle release responds more to changes in release media temperature, suggests that there is more PNIPAAM present in the chitosan-PNIPAAM co-polymer matrix. The chitosan M_w (190–310 kDa) is higher than the M_w of alginate (120–190 kDa), which may have provided more sites for NIPAAM monomer to attach and build the polymer matrix. Even though the ratios of chitosan and alginate were the same (3% w/w) to total monomers, when taking into consideration the molar ratios of NIPAAM to chitosan and alginate, one can noticed that alginate and NIPAAM will be higher than for chitosan due to their differences in molecular weight. Furthermore, different types of polymer crosslinking agents were used to form the nanoparticle micelles, based on which type of co-polymer was being used. The alginate-PNIPAAM nanoparticles were stabilized with calcium chloride, which crosslinks alginate immediately and could have potentially led to the formation

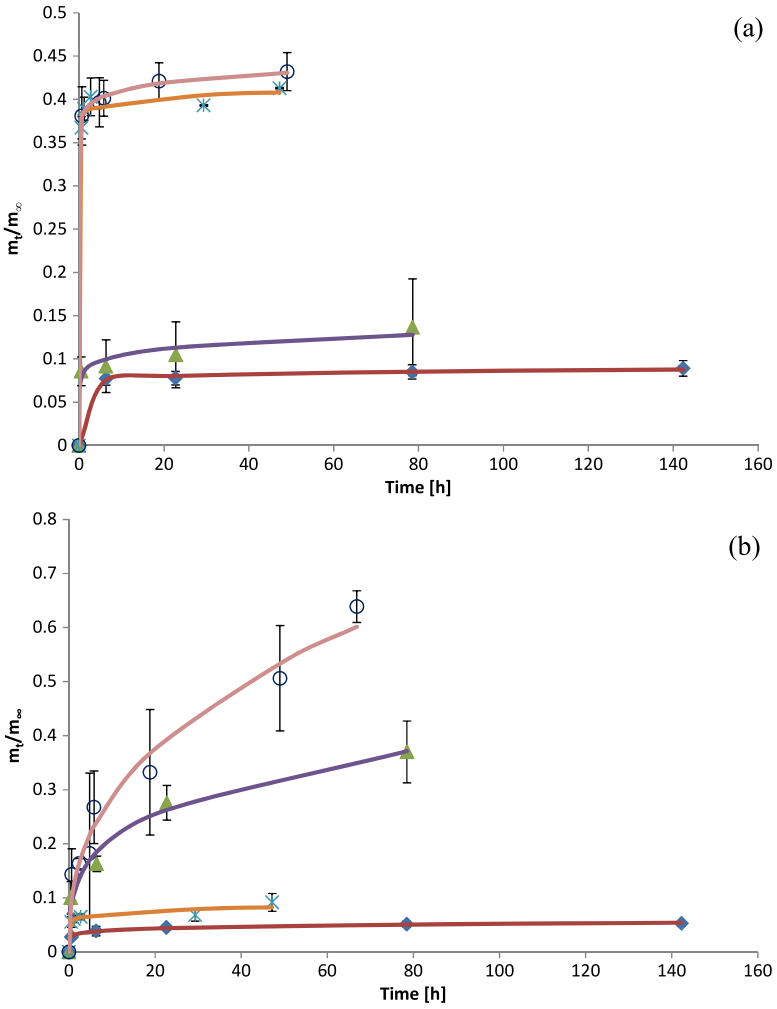

Figure 3. Controlled release profiles of (a) chitosan-PNIPAAM nanoparticles and (b) alginate-PNIPAAM nanoparticles at different temperatures in 0.15 M phosphate buffered saline (PBS) adjusted to pH 3.0 and pH 7.4, fit to model release equation (solid lines). (♦) pH 3.0 and 25 °C; (▲) pH 7.4 and 25 °C, (✳) pH 3.0 and 35 °C; (o) pH 7.4 and 35 °C. Symbols are means of 3 replicate measurements and error bars represent standard deviations.

of an exterior layer of alginate in the alginate-PNIPAAM nanoparticles. If the alginate is present on the exterior of the micelle, then its expansion or contraction will more dramatically impact the release of active material than if the PNIPAAM is expanding or contracting on the interior of the polymer micelles [34]. The chitosan-PNIPAAM micelles were crosslinked with glutaraldehyde, which crosslinks amine groups in PNIPAAM and chitosan effectively [30]. This may have led to co-polymer micelles with more heterogeneous polymer structures than those formed by the alginate-PNIPAAM polymers.

The chitosan-PNIPAAM polymer likely has a higher percentage of PNIPAAM than chitosan in its matrix, as it is the temperature-responsive component of the co-polymer, and the burst release from these particles was significantly larger at 35 °C, which is above the LCST. Above the LCST, the PNIPAAM will contract to force out a quick release of CBE before

continuing to slowly release the CBE by diffusion through the polymer matrix. The initial release of CBE is approximately four times the magnitude at 35 °C than at 25 °C, because the particle does not contract below the LCST, leaving the release to be governed primarily by diffusion. At both temperatures, the release is slightly higher when the release media is at a pH of 7.4 than pH 3.0. The chitosan polymer chains will also be contracting at pH 7.4, contributing to the initial burst release of the nanoparticles as they are added to the release media [1]. The chitosan contracts as its amine groups are deprotonated in pH environments above the pKa, causing it to be hydrophobic [34].

The alginate-PNIPAAM particle release was more significantly affected by a shift in the release media pH, indicating that this co-polymer behavior is governed primarily by alginate, the pH responsive polymer, rather than PNIPAAM. Dumitriu *et al* [29] also noted a dramatic increase in release from alginate-PNIPAAM hydrogels as the pH was increased; however, they did not measure release at different temperatures to provide a basis for the comparison in this respect. Another reason for the high rate of diffusion-governed release at pH 7.4 from alginate-PNIPAAM nanoparticles is a result of the environmental pH being well above the pKa of 3.5 for alginate. As the pH incrementally increases, the alginate molecules become highly hydrophilic and the hydrogel polymer matrix becomes swollen and opens more pores to diffusion. In contrast with the chitosan-PNIPAAM nanoparticles, the release of CBE was higher when the alginate is hydrophilic at pH 7.4 than at pH 3.0, where it is hydrophobic [5]. The burst release for these nanoparticles was much lower ($P < 0.05$) than for the chitosan-PNIPAAM nanoparticles, but the subsequent release governed by diffusion was much higher ($P < 0.05$) due to the more open nature of the polymer matrix as a swollen hydrogel [15, 29]. Lee and Chen [18] noted that the diffusion rate slowed from chitosan-PNIPAAM hydrogels as the ratio of chitosan to PNIPAAM increased as was seen in this study and explains the lower diffusion rate in the chitosan-PNIPAAM particles than the alginate-PNIPAAM particles. The release was again higher at 35 °C than 25 °C for both pHs, as the PNIPAAM contracts and contributes a burst of CBE release into the medium. Shi *et al* [31] and Moura *et al* [15] also found a similar relationship between release, temperature, and pH conditions for alginate-PNIPAAM spheres loaded with indomethacin. A previous study working with controlled release of a hydrophobic drug from chitosan-PNIPAAM particles found release profiles that were highly dependent upon the environmental pH and temperature and with a similar response to the release found in this study [27]. This study prepared chitosan-PNIPAAM co-polymer at a similar ratio of the two polymers to that which was used in the present study. Similarly, these authors showed the release of entrapped material was more impacted by a change in temperature than a change in pH. This study found that release was highest at a pH of 6.9, but there was little difference among release rates at pH values above or below 6.9 [27]. The co-polymer synthesis procedure could be refined in order to design the ratio of each stimuli-responsive component within the polymer matrix. In this way, a nanoparticle can be designed to fit a specific set of release parameters that are the most effective for antimicrobial delivery in any food system under various potential storage conditions.

The raw data from the controlled release experiments fit well to the release equation proposed for spherical, swellable polymers (equation (3)) as was expected for these nanoparticle systems (table 4). The rate coefficients and diffusion constants are slightly lower than those determined by Dumitriu *et al* [29] for a slightly more soluble encapsulated material (vanillin). All coefficients of determination (R^2) were greater than 0.95, indicating an excellent fit to the proposed release model.

Table 4. Controlled release model rate coefficients (k) and diffusion constants (n) for alginate- and chitosan-PNIPAAM nanoparticles with entrapped CBE.

		Alginate-PNIPAAM CBE			Chitosan-PNIPAAM CBE		
Temperature	pH	k_r (s^{-n})	n_r	R^2	k_r (s^{-n})	n_r	R^2
25 °C	3.0	${}_{x}1.39 \times 10^{-4} \pm 1.46 \times 10^{-5}$	${}_{x}0.55 \pm 5.05 \times 10^{-3}$	1	${}_{x}1.78 \times 10^{-4} \pm 3.59 \times 10^{-5}$	${}_{x}0.56 \pm 3.61 \times 10^{-3}$	1
	7.4	${}_{x}3.81 \times 10^{-4} \pm 6.32 \times 10^{-5}$	${}_{x}0.60 \pm 0.01$	0.99	${}_{x}2.60 \times 10^{-4} \pm 4.64 \times 10^{-5}$	${}_{x}0.58 \pm 0.01$	0.97
35 °C	3.0	${}_{x}2.83 \times 10^{-4} \pm 2.63 \times 10^{-5}$	${}_{x}0.58 \pm 4.60 \times 10^{-3}$	0.96	${}_{y}9.90 \times 10^{-4} \pm 1.76 \times 10^{-5}$	${}_{y}0.64 \pm 8.49 \times 10^{-4}$	1
	7.4	${}_{x}5.28 \times 10^{-4} \pm 1.33 \times 10^{-5}$	${}_{x}0.62 \pm 0.01$	0.97	${}_{y}6.46 \times 10^{-4} \pm 9.30 \times 10^{-5}$	${}_{x}0.62 \pm 4.02 \times 10^{-3}$	1

Values given are averages of three replicates ± standard deviations. ${}_{w}$Means within a row, of the same parameter, that are not preceded by a common subscript letter are significantly different ($P < 0.05$).

Table 5. MIC and MBC values of free CBE and CBE loaded alginate- and chitosan-PNIPAAM nanoparticles against *Salmonella enterica* Typhimurium LT2 and *Listeria monocytogenes* Scott A.

	Salmonella spp.		Listeria spp.	
Nanoparticle	MIC[1] ($\mu g\,mL^{-1}$)	MBC ($\mu g\,mL^{-1}$)	MIC ($\mu g\,mL^{-1}$)	MBC ($\mu g\,mL^{-1}$)
Alginate-PNIPAAM CBE	264[a]	>661.18[2]	397[a]	>661.18
Chitosan-PNIPAAM CBE	192[b]	>481.2	385[b]	>481.2
Free CBE*	400[c]	1000	500[c]	2000

[1]Values are the lowest concentration of nanoencapsulated CBE for which a $\leqslant 0.05$ OD630 change was observed after 24 h incubation at 35 °C in tryptic soy broth. MIC and MBC values are given based on CBE concentration.
[2]Values preceded by a higher than (>) means that tested concentrations were not sufficient to determine the MIC or MBC values.
[a]Different superscript letters within a column represent significantly different values ($P < 0.05$). Values obtained are from three independent repetitions.
*Results previously reported by [35].

3.2. Minimum inhibitory and bactericidal concentration (MIC and MBC)

The MIC values for the alginate-PNIPAAM and chitosan-PNIPAAM encapsulated CBE (table 5) were lower ($P < 0.05$) for both *S. typhimurium* and *L. monocytogenes* than the MIC values found for free CBE in a previous study (400 and 500 $\mu g\,mL^{-1}$, respectively) [35]. The MIC values for chitosan-PNIPAAM, at 192 $\mu g\,mL^{-1}$ for *S. typhimurium* and 385 $\mu g\,mL^{-1}$ for *L. monocytogenes*, were slightly lower than those found for alginate-PNIPAAM due to the inherent antimicrobial properties of chitosan. Although the control chitosan-PNIPAAM nanoparticles did not present inhibitory activity, the bacterial growth in contact with these particles was lower than the levels of growth present in either of the bacteria controls or the alginate-PNIPAAM control particles.

The MIC experiments were conducted at 35 °C and a neutral pH, so the release profiles of the antimicrobial particles would have been similar to those measured at 35 °C and pH 7.4. For the chitosan-PNIPAAM particles would have a large burst of antimicrobial as soon as the medium reached 35 °C, which would deliver a high dose of antimicrobial to the pathogens right as they are reaching their ideal growth temperature. This would increase the antimicrobial efficacy of the nanoparticles by delivering their highest dose before the bacteria is able to reach its exponential growth phase. The release profile for the alginate-PNIPAAM nanoparticles in the MIC experiment was more slow and gradual than the release of antimicrobial from chitosan-PNIPAAM nanoparticles. This slower release could contribute to the higher MIC value determined for the alginate-PNIPAAM particles. The MIC values for both nanoparticles were lower for *S. typhimurium* than for *L. monocytogenes*, because Gram-positive bacteria are less susceptible to inhibition by essential oils [36]. The antimicrobial activity of essential oils is a result of its action on the microbial cell membrane, which is more accessible to essential oils in Gram-negative bacteria [11, 36].

No MBC values were determined for these two nanoparticles, as the concentrations tested were not sufficient to kill all the bacteria present. The release of CBE was effective in preventing *S. typhimurium* than for *L. monocytogenes* growth with antimicrobial being continuously released at a concentration that allowed an inhibitory activity over time; however,

not high enough antimicrobial compounds were released initially to cause bactericidal effect. Higher concentrations of alginate or chitosan-PNIPAAM encapsulated CBE would likely result in bactericidal activity.

4. Conclusions

The antimicrobial activity found in this study shows potential for a controlled delivery system of hydrophobic antimicrobials such as essential oils that could improve their antimicrobial efficacy while minimizing their sensory impact. The release profiles of the co-polymer nanoparticles appeared to be highly dependent upon the ratio of pH and temperature-responsive polymers present in the final polymer matrix. The polymer that predominantly governs the release, determines whether the antimicrobial release is primarily affected by temperature or pH stimuli. This study shows that it is possible to engineer dual stimuli-responsive co-polymers that release antimicrobials in response to specific environmental conditions, and consequently enhance antimicrobials efficacy in adverse conditions. The results of this study showed the chitosan-PNIPAAM nanoparticles to have a higher release rate of antimicrobial material and a more effective antimicrobial activity than the alginate-PNIPAAM nanoparticles in an optimal environment for bacteria growth. In a lower temperature environment, the alginate-PNIPAAM nanoparticles would have a higher release rate than chitosan-PNIPAAM nanoparticles and potentially superior antimicrobial activity. An antimicrobial delivery system that reacts to potentially dangerous storage environments for food products could improve the food safety and prevent potentially dangerous foodborne outbreaks.

Acknowledgements

The authors would like to acknowledge Dr Taylor, Animal Science Department, Texas A&M University (TAMU) for technical assistance with MIC and MBC tests, Drs Fernando and Nikolov, Biological and Agricultural Engineering Department, TAMU, for use of lab facilities and equipment for particle size analysis and ultrafiltration, respectively.

References

[1] Rabea E I, Badawy M E, Stevens C V, Smagghe G and Steurbaut W 2003 Chitosan as antimicrobial agent: applications and mode of action *Biomacromolecules* **4** 1457–65

[2] Stossel P and Leuba J 1984 Effect of chitosan, chitin and some amino sugars on growth of various soilborne phytopathogenic fungi *J. Phytopathol.* **1** 111

[3] Leuba J and Stossel P 1986 Chitosan and other polyamines: antifungal activity and interaction with biological membranes ed R A Muzzarelli, C Jeuniaux and G W Gooday *Chitin in Nature and Technology* (New York: Plenum) pp 215–22

[4] King A H 1988 Flavor encapsulation with alginates ed S J Risch and G A Reineccius *Flavor Encapsulation. ACS Symposium Series* 370 (Washington DC: ACS Publications) pp 122–5

[5] Gu F, Amsden B and Neufeld R 2004 Sustained delivery of vascular endothelial growth factor with alginate beads *J. Control. Release* **96** 463–72

[6] Schild H 1992 Poly(*N*-isopropylacrylamide): experiment, theory and application *Prog. Polym. Sci.* **17** 163–249

[7] Gran M L 2011 Metal-polymer nanoparticulate systems for externally-controlled delivery *PhD Dissertation* The University of Texas at Austin
[8] Pelton R 2000 Temperature-sensitive aqueous microgels *Adv. Colloid Interface Sci.* **85** 1–33
[9] Sershen S, Westcott S, Halas N and West J 2000 Temperature-sensitive polymer-nanoshell composites for photothermally modulated drug delivery *J. Biomed. Mater. Res.* **51** 293–8
[10] Kalemba D and Kunicka A 2003 Antibacterial and antifungal properties of essential oils *Curr. Med. Chem.* **10** 813–29
[11] Raybaudi-Massilia R M, Mosqueda-Melgar J, Soliva-Fortuny R and Martin-Belloso O 2009 Control of pathogenic and spoilage microorganisms in fresh-cut fruits and fruit juices by traditional and alternative natural antimicrobials *Compr. Rev. Food Sci. Food Safety* **8** 157–80
[12] Valero M and Salmeron M 2003 Antibacterial activity of 11 essential oils against *Bacillus cereus* in tyndallized carrot broth *Int. J. Food Microbiol.* **85** 73–81
[13] Kim J, Marshall M and Wei C 1995 Antibacterial activity of some essential oil components against five foodborne pathogens *J. Agric. Food Chem.* **43** 2839–45
[14] Burt S 2004 Essential oils: their antibacterial properties and potential applications in foods: a review *Int. J. Food Microbiol.* **94** 223–53
[15] Moura M, Aouada A F, Favaro S L, Radovanovic E, Rubira A F and Muniz E C 2009 Release of BSA from porous matrices constituted of alginate-Ca + 2 and PNIPAAm-interpenetrated networks *Mater. Sci. Eng.* C **29** 2319–25
[16] Zhang Y, Jiang M, Zhao J, Ren X, Chen D and Zhang G 2005 A novel route to thermosensitive polymeric core–shell aggregates and hollow spheres in aqueous media *Adv. Funct. Mater.* **15** 695–9
[17] Lee C, Wen C, Lin C and Chiu W Y 2004 Morphology and temperature responsiveness-swelling relationship of poly(N-isopropylamide-chitosan) copolymers and their application to drug release *J. Polym. Sci.* A **42** 3029–37
[18] Lee W and Chen Y 2001 Studies on preparation and swelling properties of the N-isopropylacrylamide/ chitosan semi-IPN and IPN hydrogels *J. Appl. Polym. Sci.* **82** 2487–96
[19] Gomes C, Moreira R G and Castell-Perez E 2011 Poly (DL-lactide-co-glycolide) (PLGA) nanoparticles with entrapped trans-cinnamaldehyde and eugenol for antimicrobial delivery applications *J. Food Sci.* **76** N16–24
[20] Iannitelli A *et al* 2011 Potential antibacterial activity of carvacrol-loaded poly(DL-lactide-co-glycolide) (PLGA) nanoparticles against microbial biofilm *Int. J. Mol. Sci.* **12** 5039–51
[21] Zhang X Z, Wu D Q and Chu C C 2004 Synthesis, characterization and controlled drug release of thermosensitive IPN-PNIPAAm hydrogels *Biomaterials* **25** 3793–805
[22] Kim K H, Kim J and Jo W H 2005 Preparation of hydrogel nanoparticles by atom transfer radical polymerization of N-isopropylacrylamide in aqueous media using PEG macro-initiator *Polymer* **46** 2836–40
[23] Korsmeyer R W, Lustig S and Peppas N A 1986 Solute and penetrant diffusion in swellable polymers. I. Mathematical modeling *J. Polym. Sci.* B **24** 395–408
[24] Arifin D Y, Lee L Y and Wang C H 2006 Mathematical modeling and simulation of drug release from microspheres: implications to drug delivery systems *Adv. Drug. Deliv. Rev.* **58** 1274–325
[25] Brandt A L, Castillo A, Harris K B, Keeton J T, Hardin M D and Taylor T M 2010 Inhibition of *Listeria monocytogenes* by food antimicrobials applied singly and in combination *J. Food Sci.* **75** M557–63
[26] Douglas K L and Tabrizian M 2005 Effect of experimental parameters on the formation of alginate-chitosan nanoparticles and evaluation of their potential application as DNA carrier *J. Biomater. Sci., Polym. Ed.* **16** 43–56
[27] Fan L *et al* 2008 Novel super pH-sensitive nanoparticles responsive to tumor extracellular pH *Carbohydr. Polym.* **73** 390–400
[28] Ju H K, Kim S Y and Lee Y M 2001 pH/temperature-responsive behaviors of semi-IPN and comb-type graft hydrogels composed of alginate and poly (N-isopropylacrylamide) *Polymer* **42** 6851–7

[29] Dumitriu R P, Oprea A M and Vasile C 2009 Kinetics of swelling and drug release form PNIPAAm/alginate stimuli responsive hydrogels *Solid State Phenom.* **154** 17–22
[30] Chuang C Y, Don T M and Chiu W Y 2009 Synthesis of chitosan-based thermo- and pH-responsive porous nanoparticles by temperature-dependent self-assembly method and their application in drug release *J. Polym. Sci.* A **47** 5126–36
[31] Shi J, Alves N M and Mano J F 2006 Drug release of pH/temperature-responsive calcium alginate/poly (N-isopropylacrylamide) semi-IPN beads *Macromol. Biosci.* **6** 358–63
[32] Eeckman F, Amighi K and Moes A J 2001 Effect of some physiological and non-physiological compounds on the phase transition temperature of thermoresponsive polymers intended for oral controlled-drug delivery *Int. J. Food Microbiol.* **222** 259–70
[33] Verestiuc L, Ivanov C, Barbu E and Tsibouklis J 2004 Dual-stimuli-responsive hydrogels based on poly(N-isopropylacrylamide)/chitosan semi-interpenetrating networks *Int. J. Pharm.* **269** 185–94
[34] Chuang C Y, Don T M and Chiu W Y 2010 Synthesis and characteriaiton of stimuli-responsive porous/hollow nanoparticles by self-assembly of chitosan-based graft copolymers and application in drug release *J. Polym. Sci.* A **48** 2377–87
[35] Hill L E, Gomes C and Taylor M T 2013 Characterization of beta-cyclodextrin inclusion complexes containing essential oils (trans-cinnamaldehyde, eugenol, cinnamon bark, and clove bud extracts) for antimicrobial delivery applications *LWT-Food Sci. Technol.* **51** 86–93
[36] Walsh S E, Maillard J Y, Russell A, Catrenich C, Charbonneau D and Bartolo R 2003 Activity and mechanisms of action of selected biocidal agents on gram-positive and -negative bacteria *J. Appl. Microbiol.* **94** 240–7